International Cartographic Association
Association Cartographique Internationale

Dynamics of Forest Fires in P.N.N. El Tuparro: Application of Remote Sensing and Machine Learning in Environmental Monitoring.

Oscar Fernando Borda Casas [a,*]

[a] *Master student at the International University of Valencia – oscarfbordac@gmail.com*

* Corresponding author

Abstract: Forest fires are among the leading causes of sudden vegetation cover loss, originating from natural phenomena or human-induced activities. These events are significant ecological disturbances that can severely alter ecosystem structure, degrade soil properties, and disrupt natural regeneration processes. In Colombia's El Tuparro National Natural Park (P.N.N. El Tuparro), fire dynamics are strongly influenced by climatic variability and land-use practices. This study addresses the need for precise monitoring tools to assess the impact of wildfires in protected areas. We used multi-temporal Landsat imagery (2013–2023) and supervised classification with Support Vector Machines (SVM) to detect and quantify burned areas. A set of spectral indices (NDVI, NBR, SAVI, NDWI) was calculated to evaluate fire severity and vegetation recovery. Results reveal a strong relationship between fire events and reductions in vegetation vigor and biomass, with grassland ecosystems showing the highest resilience. Anomaly detection using the Isolation Forest algorithm identified extreme fire-related events and climatic anomalies. These findings emphasize the importance of continuous vegetation monitoring and the development of mitigation strategies to reduce wildfire impacts in vulnerable ecosystems.

Keywords: Forest fires, Remote sensing, Spectral indices, Machine learning.

1. Introduction

Understanding the severity of forest fires is essential due to their numerous negative impacts, such as air quality deterioration, increased greenhouse gas emissions, changes in soil fertility, and biodiversity loss (Belenguer-Plomer et al., 2019; Hansen et al., 2013; Van der Werf et al., 2010; Aponte et al., 2016; Bond et al., 2005; Pausas and Paula, 2012). Wildfires are among the leading causes of sudden vegetation cover loss globally and may result from both natural processes and human activities (Chen et al., 2013; Bond & Keane, 2017). Their occurrence is influenced by factors such as drought, precipitation variability, wind, and climate phenomena like El Niño (Van der Werf et al., 2010). Fire severity depends on the amount of biomass consumed, which is determined by vegetation type and climatic conditions, and can be estimated using spectral indices such as the differenced Normalized Burn Ratio (dNBR) (Keeley, 2009). In this context, P.N.N. El Tuparro has experienced a high frequency of forest fires over the past decade. According to Orlando Molano, former P.N.N. director, approximately 71,000 hectares were affected by fires in 2021, while in 2013 and 2014, approximately 160,000 hectares and almost 200,000 hectares were burned, respectively. These data suggest that around 50% of El Tuparro National Natural Park has a high probability of being affected by fires.

Several recent studies have examined land cover dynamics and fire monitoring in this region. Cortes & Zorro (2023) found overall land cover stability between 2013 and 2023, although they reported an estimated 10% loss of forested area. The park's Management Plan (Patiño et al., 2007) identifies a clear seasonal pattern, with an increase in fires during the dry season (December to March) and vegetation recovery during the rainy season (April to November). Eraso et al. (2022) demonstrated the utility of remote sensing using Sentinel-2 imagery and the NBR index within Google Earth Engine (GEE), while Velasco (2021) employed machine learning classifiers (Random Forest) with Sentinel-2 data to estimate post-fire severity, improving classification accuracy. Despite these advances, a knowledge gap remains in the monitoring of fire dynamics and vegetation recovery in Colombia's protected areas, particularly through the combined use of advanced remote sensing and machine learning algorithms. Although the impact of wildfires has been widely documented internationally (Roteta et al., 2019), site-specific applications remain limited. The use of geospatial data has facilitated more detailed monitoring of fire-affected areas, as well as the assessment of fire severity and post-fire recovery through spectral indices (Lizundia et al., 2020). Furthermore, machine learning algorithms have proven effective in identifying and classifying affected areas.

In this context, the present study analyzes the severity and temporal dynamics of wildfires in P.N.N. El Tuparro from 2013 to 2023, using Landsat satellite imagery and supervised classification with Support Vector Machines (SVM) to map burned areas. Time series analyses were applied to assess vegetation recovery, and the Isolation Forest algorithm was implemented to detect anomalies. Finally, surface temperature trends were examined to identify climatic patterns associated with fire occurrence. This methodological approach enables the quantification of damage and the identification of spatiotemporal patterns, providing key information for the sustainable management of tropical protected ecosystems.

2. Methodology

For this work, the following methodology was used:

2.1 Study Area:

The study area corresponds to P.N.N. El Tuparro, identified as one of the most fire-affected regions in Colombia based on analysis from platforms such as NASA's FIRMS and WORLDVIEW. The boundary of this area is presented in Figure 1.

This natural park is located in the eastern part of Colombia and is characterized by alternating periods of drought and rainfall, with temperatures ranging between 18 and 36°C and annual precipitation between 1500 and 1900 mm. This region is composed of savannahs located on the bed of the Meta River and equipped with an independent hydrological network. This allows these savannas to avoid flooding during the rainy season, unlike those located on the left bank of the river.

It is estimated that less than 3% of this subregion, which holds agricultural, livestock, and forestry potential, is currently used for these purposes. This is due to factors such as its low fertility (high acidity, high aluminum saturation, low organic matter and phosphorus content) and the pronounced dry season between December and March. The data used to create the map in Figure 1 were extracted from the National Geo-statistical Framework (MGN) of DANE.

2.2 Analysis Process

This study employed multiple remote sensing tools and image processing techniques integrated with machine learning algorithms. The workflow was as follows:

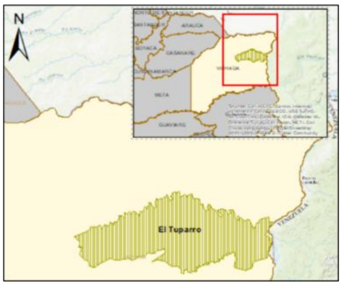

Figure 1. Study area location. Source: Data obtained from DANE.

2.2.1 *Information and Input Acquisition*

Satellite images from Landsat 8 and 9 (from 2013 to 2023) with less than 10% cloud cover were used from the EarthExplorer platform. The images were preprocessed with atmospheric correction (ATCOR) and pan-sharpening (NNDifuse) to improve their quality and spatial resolution. They were then cropped to the study area and 17 mosaics were generated, ready for classification.

2.2.2 *Classifications*

A representative image from March 2017 was selected due to its cloud-free condition and variety of land cover types. Pixel-based classification methods were employed using machine learning algorithms (SVM, Random Forest, and KNN). The best method was evaluated and applied to the entire set of images.

2.2.3 *Burned Area Estimation*

Burned area estimation was performed using the best classifier algorithm out of the three proposed. Land covers such as rivers, grasslands, forests, and burned areas were identified. Landsat images proved to be suitable for this analysis, achieving over 80% accuracy in the estimations.

2.2.4 *Calculation of Spectral Indices*

Indices such as NDVI, SAVI, NBR, NBR2, and NDWI were calculated to evaluate vegetation and burned areas. Additionally, dNBR was used to estimate fire severity by comparing pre- and post-fire indices. The results were consolidated into a spectral indices data cube.

2.2.5 *Evaluation of Burned Area Recover*

Two polygons with moderate to high burn severity were analyzed by calculating medians of NDVI, SAVI, NBR, NBR2, and NDWI indices. Time series were generated with GEE, revealing specific recovery patterns. The Isolation Forest algorithm detected anomalies in the recovery process.

Advances in Cartography and GIScience of the International Cartographic Association, 5, 5, 2025.
32nd International Cartographic Conference (ICC 2025), 17–22 August 2025, Vancouver, Canada. This contribution underwent double-blind peer review based on the full paper. https://doi.org/10.5194/ica-adv-5-5-2025 |

2.2.6 *Temperature Anomalies and Trend*

Surface temperature time series were generated using MODIS data (MOD11A2) downloaded from GEE. Trends were analyzed using statistical models (linear regression, Mann-Kendall, Dickey-Fuller), and anomalies were detected through the Isolation Forest algorithm. This analysis assessed the impact of fires on temperature changes.

3. Results

The results of this study are presented below:

3.1 Information and Input Acquisition

The study was based on the acquisition of Landsat 8 and 9 satellite images available between 2013 and 2023. A total of 34 images with less than 10% cloud cover were selected to ensure quality and minimize omissions in surface cover. This limited the availability of images for certain months, so dates close to each other were prioritized to avoid significant variations in spectral indices. Finally, 17 mosaics were generated from the selected images.

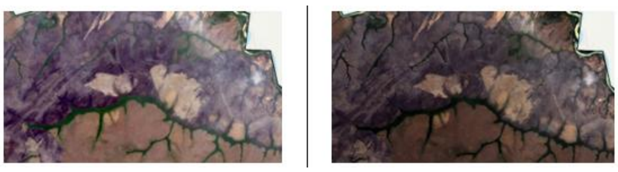

Figure 2. Comparison between Original and Atmospherically Corrected Image of LC08_L1TP_004056_20140222_20200911_02_T1.

The images were processed using Catalyst software, applying atmospheric correction at the surface level through the "ATCOR - Ground Reflectance" tool (Figure 2). Subsequently, the spatial resolution was improved from 30 meters to 15 meters using the pansharpening technique nnDifuse in ENVI, based on a nearest neighbor diffusion model (Figure 3).

Figure 3. Comparison between Original and Pansharpened Image of LC08_L1TP_004056_20140222_20200911_02_T1

Finally, mosaics were generated in Catalyst to integrate image pairs with insufficient individual coverage (Figure 4).

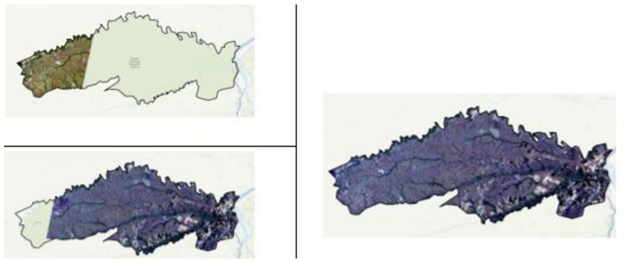

Figure 4. Final Mosaic of LC08_L1TP_005056_20140112_20200912_02_T1 and LC08_L1TP_004056_20140121_20200912_02_T1 Images.

3.2 Classifications

Pixel-based classifications were implemented using Orfeo Toolbox tools (QGIS) with algorithms such as SVM (linear, RBF, polynomial, and sigmoid), Random Forest, and KNN. The classes or land covers to be classified are shown in Figure 6.

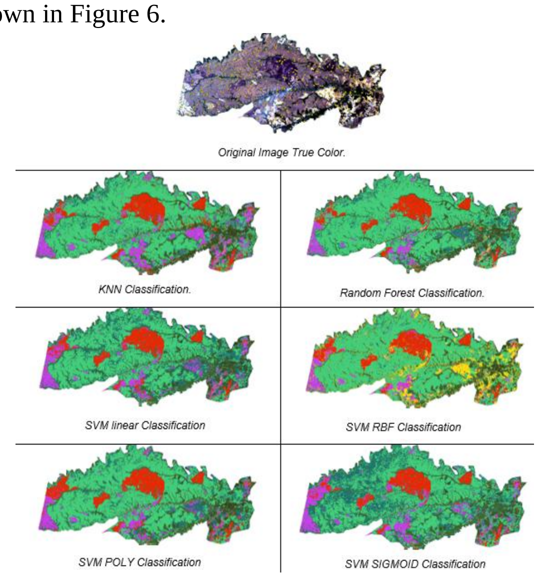

Figure 5. Comparison between the results of general classifications in OTB QGIS.

Visual results showed similar spatial distributions, although there were differences in the classification of certain land covers. An example of this is sandy areas, which were overestimated by the SVM RBF algorithm (Figure 5).

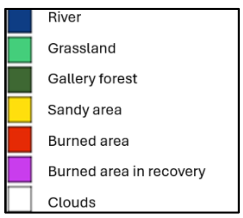

Figure 6. Land Covers

3.3 Classification Evaluation

To evaluate the classifications, 316 reference samples were randomly distributed across the study area (Figure 7). This generated confusion matrices, and metrics such

 https://doi.org/10.5194/ica-adv-5-5-2025 |

as overall accuracy, recall, F1-score, and Kappa index were calculated (Table 1).

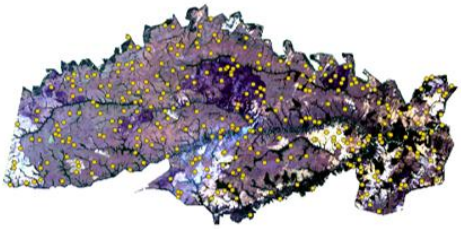

Figure 7. Comparison of Classification Results Generated in OTB QGIS

The results showed significant variability in the performance of the classification algorithms based on the different land covers evaluated. Algorithms such as linear SVM and Random Forest performed well in four of the six classes analyzed, although limitations were observed in the classification of "sandy areas" and "recovery areas." These difficulties suggest the need for adjustments in the model parameters to improve accuracy. Additionally, the selection of the kernel was a determining factor in the performance of the SVM algorithms, significantly affecting the quality of the obtained classifications.

In terms of recall, the Random Forest and linear SVM algorithms achieved high values in most land covers, indicating their effectiveness in identifying positive instances. However, the SVM RBF and SVM sigmoid algorithms exhibited poor performance in the "sandy areas" class, possibly due to the low spectral differentiation of the samples.

The analysis of the F1-score confirms the overall effectiveness of the Random Forest and linear SVM algorithms, with values exceeding 75% in most classes. However, difficulties were observed in the "sandy areas" class for the SVM RBF and SVM sigmoid algorithms, with F1-scores of 0.17 and 0.00, respectively. In contrast, linear SVM demonstrated better performance in this class, with an F1-score of 0.75, highlighting it as a good option for identifying these areas.

Algorithm	General Accuracy	Kappa Index
Random forest	0.900	0.844
KNN	0.833	0.755
SVM linear	0.906	0.863
SVM poly	0.893	0.839
SVM rbf	0.810	0.724
SVM sigmoid	0.859	0.801

Table 1. Evaluation of General Accuracy and Kappa Index of the Classifications.

The evaluation of overall accuracy and the Kappa index (Table 1) shows linear SVM as the best classifier, with an overall accuracy of 90.6% and a Kappa index of 0.863. Random Forest also showed competitive performance, achieving an overall accuracy of 90% and a Kappa index of 0.844. In contrast, SVM RBF obtained the lowest values, reflecting a lower agreement between predicted and observed classifications.

These findings highlight the importance of conducting a multidimensional analysis considering metrics such as accuracy, recall, and F1-score to comprehensively evaluate the performance of classifier models. They also underscore the need to select algorithms that adapt to the specific characteristics of the analyzed land covers. In this regard, linear SVM not only achieved the best results in terms of accuracy and consistency but also demonstrated a suitable ability to differentiate between classes.

3.4 Estimation of Burned Areas

Sampling was conducted using images from Landsat 8 and 9 satellites, which served as the basis for creating training files using the linear SVM model. This model was employed to perform classifications across various time periods.

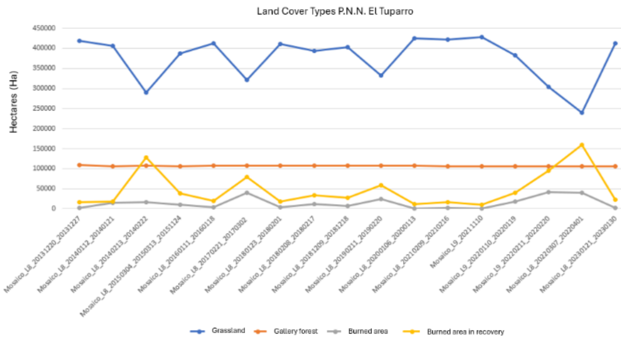

Figure 8. Variation in the amount of hectares of the coverages from 2013 to 2023.

The results show the distribution and quantification of land covers in the PNN El Tuparro, highlighting the dynamics of major categories such as herbaceous, gallery forest, burned areas, and recovery areas. This data was complemented with the generation of a time series (Figure 8) spanning from 2013 to 2023, allowing for the observation of cover variations over the course of a decade.

The analysis reveals that herbaceous land is the most extensive vegetation cover in the park, showing significant variations in its area. This suggests that this ecosystem is highly sensitive to both environmental factors and human activities. On the other hand, the gallery forest exhibited relative stability over time. However, a slight decrease of approximately 2900 hectares in its extent was observed during the study period. This decline may be related to pressures such as climate change and human activities expanding other land covers. A crucial aspect of the park's dynamics is the occurrence of fires, evidenced by the increase in areas classified as "burned" and "in recovery." These events, along with climate variability and fire management, significantly influence the composition and structure of vegetation. For instance, herbaceous areas are particularly affected, reflecting their high vulnerability to these disturbances, but despite this, a recovery trend is identified.

It is important to note some observations that external factors such as the presence of clouds or shadows in the images may affect classification, introducing uncertainties in the results. These limitations should be considered when interpreting the observed variations and in future studies focused on the dynamics of the ecosystems in PNN El Tuparro.

3.5 Calculation of Spectral Indices

At this stage, Orfeo Toolbox (OTB) tools were used to develop a Python script that allowed for the calculation of various spectral indices, including NDVI, SAVI, NBR, NBR2, and NDWI. These indices were employed to assess the recovery of vegetation through their values across different time periods.

Symbol	Range	Severity Level
	< -0,25	High post-fire vegetation growth
	-0,25 – – 0,1	Low post-fire vegetation growth
	-0,1 – 0,1	Stable or unburned areas
	0,1 – 0,27	Burned areas with low severity
	0,27 – 0,44	Burned areas with moderate-low severity
	0,44 – 0,66	Burned areas with moderate-high severity
	> 0,66	Burned areas with high severity

Figure 9. Categorization of severity based on the dNBR index, proposed by USGS.

With the already generated NBR indices, 16 dNBR indices for fire events were calculated. The thresholds used to classify fire severity correspond to those established by the USGS (España et al., 2024), which are shown in Figure 9. An example of fire severity calculated using dNBR can be seen in Figure 10.

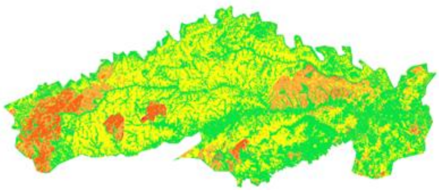

Figure 10. Example of dNBR for Mosaico_L9_20211110.

Vegetation recovery monitoring has ecological implications, playing an important role in resource management and the prevention of future fires. Identifying areas with lower recovery capacity helps direct restoration and conservation efforts, ensuring the sustainability of the ecosystems in the P.N.N. El Tuparro.

3.6 Evaluation of Burned Area Recovery

Vegetation recovery was assessed using the previously calculated Burned Area Index (dNBR) values. In the analysis, two representative zones with different severity levels were identified, distributed throughout the study area (Figure 11).

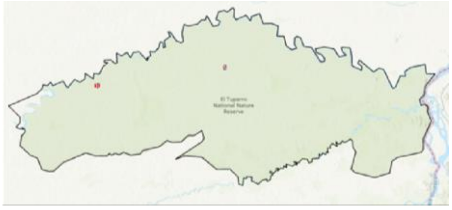

Figure 11. Location of the 2 study zones. Source: Self-made.

For each of these zones, zonal statistics were extracted from a set of spectral indices: NBR, NBR2, NDVI, SAVI, and NDWI. The indices used were concatenated into a multitemporal data cube, combining multiple previously processed satellite images. This allowed the evaluation of vegetation recovery trends based on the different severities of the fires.

a) Polygon 1:

Four fire events with variable severities were identified. The most severe event occurred in January 2014 (Figure 12), with a severity classified as moderate-high. In the other dates, the severity was moderate-low.

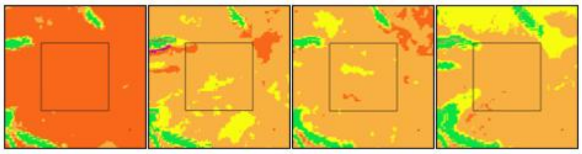

Figure 12. Visualization of the four dates where fire severity ranged from moderate-low to moderate-high: a) January 2014, b) February 2017, c) February 2019, and d) January 2022.

The results showed seasonal patterns in the indices (Figure 13), associated with the natural growth cycles of vegetation. However, four periods of significant decline in NDVI values were identified, reaching values below 0.3, which coincide with the fire events, indicating a notable loss of vigor and water content in the vegetation. In January 2014, during the most severe event, the NBR index sharply decreased to values close to -0.3, reflecting the effects of the wildfire. At this time, the vegetation showed a high level of damage, with significantly reduced density and moisture content. The low values of the indices confirmed that the vegetation was severely stressed, with predominantly dry conditions.

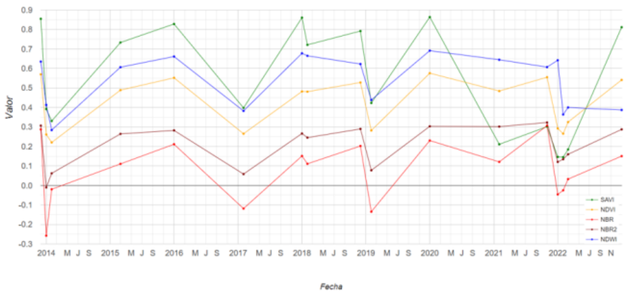

Figure 13. Time series of spectral indices from 2013 to 2023 in Polygon 1.

In the other fire dates, the spectral indices also showed the evident impacts of the fire. The low NDVI and SAVI values reflected a decrease in photosynthetic activity and live vegetation coverage. In parallel, the NBR and NBR2 indices indicated significant biomass loss, while the low NDWI values suggested a reduction in soil and vegetation moisture content. These indicators signaled that the vegetation was in a recovery phase, with limited water and biomass availability. Despite the severe impacts of the fires, notable recovery in the vegetation was observed, probably attributed to the dominance of herbaceous vegetation in the area, which has high regrowth capacity. The NDVI values showed recovery, reaching levels similar to those prior to the event in approximately one year.

	Tiempo	SAVI_P1	SAVI_std	NDVI_P1	NDVI_std	NBR_P1	NBR_std
1	2014-01-01	0.391964	0.015633	0.261435	0.010437	-0.257716	0.013868
2	2014-02-01	0.330438	0.034907	0.220332	0.022928	-0.019601	0.025262

	NBR2_P1	NBR2_std	NDWI_P1	NDWI_std	Tiempo_num	anomaly
1	-0.010137	0.031100	0.413006	0.010772	31	-1
2	0.061888	0.010531	0.283956	0.015354	62	-1

Figure 14. Dates detected as anomalies within the analysis of polygon 1.

To complement this analysis, the IsolationForest algorithm was used, which identified anomalies in the indices for January and February 2014 (Figure 14). These findings matched the visual and numerical analysis of the time series, confirming the high severity of the fires during that period and the abrupt changes in the spectral indices. In summary, the fires in this area, especially the one in January 2014, caused a significant decrease in vegetation biomass and moisture content, increasing soil exposure. However, the rapid recovery observed highlights the resilience of the herbaceous vegetation in the area, which was able to restore itself in a relatively short period.

b) Polygon 2:

In this area, a fire event was identified in January 2022, with severity levels ranging from moderate-high (dark orange) to high severity (purple). The most significant impact was located towards the upper left of the area (Figure 15).

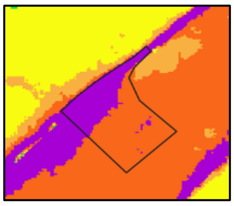

Figure 15. Visualization of the fire severity in January 2022 (moderate-high severity).

The analysis of the time series shown in Figure 16, covering the period from 2014 to 2022, revealed normal seasonal fluctuations in vegetation. During this period, vegetation indices showed higher values during growth periods and expected declines during dry seasons. The NBR index consistently showed positive values above 0.07, indicating the absence of large-scale fires until the event in 2022.

Figure 16. Time series of spectral indices from 2013 to 2023 in Polygon 2.

January 2022, marked by the occurrence of the fire, represented a turning point in the time series. During this period, all spectral indices showed a significant decline. The NBR index dropped to negative values of approximately -0.3, reflecting the severity of the burn and vegetation loss. Consistently, the NDVI and SAVI indices also decreased, indicating a loss of biomass and vigor in the vegetation. On the other hand, although the NDWI index also declined, the drop was not as pronounced. In the months following the event, the indices began to show recovery. The NBR index returned to positive values, indicating the absence of new fires. However, the recovery of biomass, as represented by the SAVI index, was slower compared to the NDVI, which showed a quicker improvement in vegetation vigor. By 2023, significant recovery was observed, especially in terms of biomass.

The complementary analysis using the IsolationForest algorithm identified the months of January and February 2022 as anomalies (Figure 17). The anomaly in January is directly attributed to the fire impact, evidenced by the abrupt changes in the index values. For instance, the NDVI dropped from 0.58 to 0.08, while the SAVI index decreased from 0.3 to 0.02.

	Tiempo	SAVI	SAVI_std	NDVI	NDVI_std	NBR	NBR_std
13	2022-01-01	0.234708	0.031394	0.450447	0.049262	0.163008	0.065209
14	2022-02-01	0.181140	0.029845	0.353018	0.046375	0.049403	0.068984

	NBR2	NBR2_std	NDWI	NDWI_std	Tiempo_num	anomaly
13	0.298019	0.017241	0.647448	0.020408	2953	-1
14	0.266208	0.017998	0.464978	0.024602	2984	-1

Figure 17. Dates detected as anomalies in the analysis of Polygon 2.

The anomaly detected in February 2022 is explained by a particular behavior: while the NDVI, SAVI, and NBR indices showed slight increases, the NDWI index decreased. This suggests a possible loss of moisture in the soil, probably as a residual effect of the fire that occurred the previous month. In summary, the January 2022 event had a significant impact on vegetation, with a marked reduction in biomass and vigor, as well as a moderate effect on soil moisture. The recovery observed in 2023 highlights the vegetation's resilience, although some variability in the response of the different indices remains.

The spectral index analysis in the two study polygons allowed the identification and quantification of how wildfires affect vegetation. The results showed clear patterns in vegetation's response to these events. Areas

 https://doi.org/10.5194/ica-adv-5-5-2025 |

covered by herbaceous vegetation exhibited a remarkable ability to regenerate, likely due to their capacity for rapid regrowth. Additionally, the use of the IsolationForest algorithm effectively detected the fires as anomalies in the spectral data, which validated the findings obtained from the time series analysis and numerical data.

3.7 Evaluation of Anomalies and Trends in Surface Temperature

To evaluate trends and anomalies in surface temperature, as well as their relationship with events such as wildfires, MODIS sensor data from Google Earth Engine (GEE) were used.

Figure 18. Time series of surface temperature from MODIS in GEE.

A time series from 2013 to 2023 was generated (Figure 18), though there were some discontinuities due to missing data in certain intervals. The data was processed in Python and grouped monthly for easier analysis.

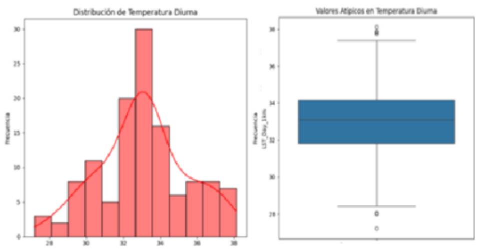

Figure 18. Dates detected as anomalies within the analysis of Polygon 2.

The descriptive analysis revealed significant differences between daytime temperatures (average of 33.1°C) and nighttime temperatures (average of 22.8°C). The distribution of daytime temperatures showed greater variability and a slight positive skew, with values concentrated between 32-34°C. These differences reflect the impact of climatic factors such as solar radiation and humidity. The Shapiro-Wilk test was performed to validate the normality of the data, and it was found that the daytime temperature data had a statistic (0.98) below the critical value (p-value = 0.11), suggesting that the null hypothesis cannot be rejected, i.e., there is insufficient evidence to claim that the temperature data deviates significantly from a normal distribution.

To determine a potential trend in the data, the Mann-Kendall test was used. Upon analyzing the results (Figure 19), no significant trend was found in either daytime or nighttime temperatures. Although the Mann-Kendall statistics are positive, suggesting a very slight upward trend, the lack of statistical significance (high p-values) suggests that there is insufficient statistical evidence to conclude that a significant trend exists in the data.

Mann-Kendall statistic: 0.309
p-value: 0.213
No significant trend was found.

Figure 19. Results of the Mann-Kendall test.

As a final step to determine the presence of an upward trend or seasonality in the temperature data, the Augmented Dickey-Fuller test was conducted (Figure 20). For daytime temperature, the p-value obtained was 0.1537, which exceeds the standard threshold of 0.05, and although the ADF statistic is negative, it is not low enough to reject the null hypothesis. This suggests that the daytime temperature series is likely non-stationary. The statistical tests implemented showed that daytime temperatures have an approximately normal distribution but are non-stationary, with short-term variation patterns.

	Fecha	LST_Day_1km
12	2014-01-01	34.47525
13	2014-02-01	38.11750
14	2014-03-01	37.74975
17	2014-06-01	28.54900
18	2014-07-01	28.42700
29	2015-06-01	28.00050
30	2015-07-01	28.04950
62	2018-03-01	37.17250
66	2018-07-01	27.19225
73	2019-02-01	37.89375
74	2019-03-01	37.33900
85	2020-02-01	37.39400
86	2020-03-01	37.84150

Figure 20. Detected surface temperature anomalies from 2013 to 2023.

The Isolation Forest algorithm was used to detect 13 anomalous dates in the surface temperatures, grouped into two critical seasons. Between January and March, daytime temperatures increased by more than 2°C due to intense wildfires, exacerbated by the El Niño phenomenon. Between June and July, a decrease of more than 9°C was observed, related to the La Niña phenomenon, characterized by increased cloud cover and precipitation. These results highlight the influence of global climate cycles on the thermal conditions of the study area.

Continuous monitoring of surface temperature is crucial for identifying extreme events and assessing their impact on local ecosystems, enabling better management and planning of conservation actions.

4. Conclusions

From the methodological process implemented in this research, the following conclusions are derived:

Estimation of Burned Areas: The application of the SVM algorithm with a linear kernel proved to be an effective tool for classifying vegetation cover in the P.N.N. El Tuparro, with an accuracy close to 90%. This allowed for the detailed identification and quantification of areas affected by wildfires, validating the potential of machine learning models in remote sensing studies.

Spectral Index Analysis: The combined use of indices such as NDVI, NDWI, SAVI, NBR, and NBR2, along with dNBR, allowed for the evaluation of vegetation dynamics after wildfires. This approach revealed clear patterns of gradual recovery in the analyzed polygons, depending on fire severity, vegetation type, and climatic conditions. These findings highlight the importance of continuous monitoring for the sustainable management of affected ecosystems.

Anomaly Detection: The implementation of the Isolation Forest algorithm was crucial for detecting anomalies in vegetation and surface temperature time series. These anomalies reflected the direct impact of severe wildfires and climatic variations, emphasizing the relevance of a multitemporal and multidimensional approach to understanding ecosystem dynamics.

Relationship Between Fires and Climate: The analyses revealed thermal anomaly patterns between January and March, associated with high temperatures and increased wildfire occurrences, while between June and July, thermal decreases were observed linked to wetter seasons. These results underscore the interaction between wildfires and climatic conditions, providing crucial information for environmental planning.

In summary, this research provides a comprehensive view of vegetation dynamics in the P.N.N. El Tuparro, highlighting the influence of wildfires and climatic conditions on its health and recovery from 2013 to 2023. The findings emphasize the need for continuous monitoring that combines remote sensing, temporal analysis, and advanced machine learning techniques to support the sustainable management of natural resources.

5. References

Aponte, C., de Groot, W.J. & Wotton, B.M. (2016). Forest fires and climate change: causes, consequences and management options. *International Journal of Wildland Fire*, vol. 25, pp. 1-2.

Belenguer-Plomer, M.A., Tanase, M.A., Fernandez-Carrillo, A. & Chuvieco, E. (2019). Burned area detection and mapping using Sentinel-1 backscatter coefficient and thermal anomalies. Remote Sensing of Environment, vol. 233, 111345.

Bond, W.J., Woodward, F.I. & Midgley, G.F. (2005). The global distribution of ecosystems in a world without fire. *New Phytologist*, vol. 165, pp. 525–538.

Bond, W., & Keane, R. (2017). Fires, Ecological Effects of. Elsevier. ACM SIGSPATIAL GIS'17, November 2–5, 2017, San Jose, California, pp. 1–11.

Chen, M. D. (2013). Long-term trends and interannual variability of forest, savanna, and agricultural fires in South America. Future Science, pp. 617–638.

Cortes, C. & Zorro, D., 2023. Análisis de cambio de coberturas de la tierra durante el periodo 2000 – 2023 en el Parque Nacional Natural El Tuparro, departamento del Vichada, Colombia. *Bogotá*.

Eraso, O., Badia, A., & Gisbert, M., 2022. Google Earth Engine aplicado al monitoreo de superficies quemadas y cambios de coberturas y usos del suelo. *GeoFocus, Revista Internacional de Ciencia y Tecnología de la Información Geográfica*, pp. 89-113.

España, M., Champo, O., & Uribe, D. (2024). Extensión y severidad de incendios forestales en Michoacán en 2021 a partir de imágenes Sentinel-2. Polibotánica. ACM SIGSPATIAL GIS'24, November 2–5, 2024, San Jose, California, pp. 125–144.

Hansen, M.C., Potapov, P.V., Moore, R., Hancher, M., Turubanova, S., Tyukavina, A., Thau, D., Stehman, S., Goetz, S., Loveland, T. (2013). High-resolution global maps of 21st-century forest cover change. *Science*, vol. 342, pp. 850–853.

Keeley, J. (2009). Fire intensity, fire severity, and burn severity: A brief review and suggested usage. International Journal of Wildland Fire. ACM SIGSPATIAL GIS'09, November 2–5, 2009, San Jose, California, pp. 116–126.

Lizundia, J., Otón, G., Ramo, R., & Chuvieco, E. (2020). A spatio-temporal active-fire clustering approach for global burned area mapping at 250 m from MODIS data. Remote Sensing of Environment. ACM SIGSPATIAL GIS'20, November 2–5, 2020, San Jose, California.

Patiño, O., Berman, E., Villarraga, A., Rodríguez, A., Rodríguez, J., Ramírez, R., and Alvarado, B., 2007. Plan de Manejo del Parque Nacional Natural El Tuparro 2007–2012. Instituto Alexander von Humboldt, Bogotá, Colombia.

Pausas, J.G. & Paula, S. (2012). Fuel shapes the fire-climate relationship: evidence from Mediterranean ecosystems. *Global Ecology and Biogeography*, vol. 21, pp. 1074–1082.

Soler, D., & Hernández, P. (2018). Desarrollos y perspectivas de investigación en la Orinoquía. *Revista de Medicina Veterinaria*, pp. 7-13.

Roteta, E., Bastarrika, A., Padilla, M., Storm, T., & Chuvieco, E., 2019. Development of a Sentinel-2 burned area algorithm: Generation of a small fire database for sub-Saharan Africa. *Remote Sensing of Environment*, pp. 1-17.

Van der Werf, R. J. (2010). Global fire emissions and the contribution of deforestation, savanna, forest, agricultural, and peat fires. Atmospheric Chemistry and Physics. ACM SIGSPATIAL GIS'10, November 2–5, 2010, San Jose, California, pp. 11707–11735. doi:10.5194/acp-10-11707-2010.

Velasco, R., 2021. Aplicación de teledetección para estimación de severidad post-incendio. *Valladolid: Universidad de Valladolid*.